Journal of Ceramic Processing Research. Vol. 13, No. 3, pp. 210~214 (2012)

J O U R N A L O F
Ceramic Processing Research

Au-assisted growth, Raman spectra, and photoluminescence of Mg_2SiO_4 nanowires

Han Gil Na[a], Tran Van Khai[a], Dong Sub Kwak[a], Yong Jung Kwon[a], Kwang Bo Shim[a], Sung Soo Kim[b], Hyeonsik Cheong[b] and Hyoun Woo Kim[a,*]

[a]*Division of Materials Science and Engineering, Hanyang University, Seoul 133-791, Republic of Korea*
[b]*Department of Physics, Sogang University, Seoul 121-742, Republic of Korea*

We have prepared Mg_2SiO_4 nanowires by a thermal heating method with Au-coated substrates gathering the products. We investigated the effect of the Au layer thickness on the nanowire morphology using scanning electron microscopy, suggesting a possible growth mechanism of Mg_2SiO_4 nanowires. XRD spectra and lattice-resolved TEM images indicated that the nanowires had an orthorhombic Mg_2SiO_4 phase. For the first time, we report the Raman and photoluminescence (PL) spectra of Mg_2SiO_4 nanowires. Raman lines corresponding to the SiO_4 group from Mg_2SnO_4 were observed. The PL measurement with a Gaussian fitting exhibited visible light emission bands centered at 2.03, 2.21, 2.45, and 2.95 eV.

Key words: Nanowires, Mg_2SiO_4, Au layers.

Introduction

In recent years, various nanostructures have been intensively studied for possible application in future nanodevices [1-10]. Among them, one-dimensional (1D) nanostructures, including nanowires, have attracted special attention due to their distinctive geometries, novel physical and chemical properties, and promising applications in numerous areas including nanoscale electronics and photonics [11, 12].

Forsterite (Mg_2SiO_4) is a member of the olivine family of crystals. It has an orthorhombic crystal structure in which Mg^{2+} occupies two nonequivalent octahedral sites: one (M1) with inversion symmetry (C_i) and the other (M_2) with mirror symmetry (C_s) [13,14]. Since Mg_2SiO_4 is one of the main constituents of the lower crust of the Earth, it determines crucial geophysical properties of the Earth's interior such as possible phase transitions and the thermodynamics of rock-forming minerals [15]. Furthermore, its interesting and peculiar properties suggest future industrial applications. Its refractory nature makes it suitable for use in thermal insulation [16, 17]. Chromium-doped Mg_2SiO_4 has been shown to be a promising active medium for a tunable laser [18, 19]. Accordingly, 1D nanostructures of Mg_2SiO_4 will find a variety of applications in future nanodevices.

In spite of its importance, there have been a few reports on the fabrication and properties of Mg_2SiO_4 nanostructures. Zhang et al. reported the self-assembled in plane growth of Mg_2SiO_4 nanowires [20]. Xie et al. studied the formation mechanism of Mg_2SiO_4 fishbone-like fractal nanostructures [21]. In addition, Whitby et al. produced leaf-like Mg_2SiO_4 nanostrctures via iodine vapour transport of magnesium onto quartz substrates [22].

In a previous study, we have reported initial data on the fabrication of Mg_2SiO_4 nanowires [23]. In the present paper, with the expectation that the thickness of a pre-deposited Au layer on a Si substrate will affect the product morphology, we have varied the thickness in the range of 3-120 nm. For the first time, we present the Raman and photoluminescence (PL) spectra of Mg_2SiO_4 nanowires.

Experimental

The method of preparation of nanowires has been previously described [23]. Au-coated substrates were placed in an alumina boat, which was located in the middle of a quartz tube. The quartz tube was inserted into a horizontal tube furnace. In order to investigate the effect of the thickness of the pre-deposited Au layer, we have set the thickness to 3, 10, 40, and 120 nm.

We aimed at synthesizing nanowires of the Mg_2SiO_4 phase. The source of Si was the Si substrate. The primary source of O was oxygen in the ambient gas flow. Also, a possible source of Mg is the pre-coated MgO layer on the inner surface of the quartz tube. It is surmised that the inner surface of the quartz tube had been coated with a thin MgO layer, by means of the thermal evaporation of MgB_2 powder during the

*Corresponding author.
Tel: +82-10-8428-0883
Fax: +82-2-2220-0389
E-mail: hyounwoo@hanyang.ac.kr

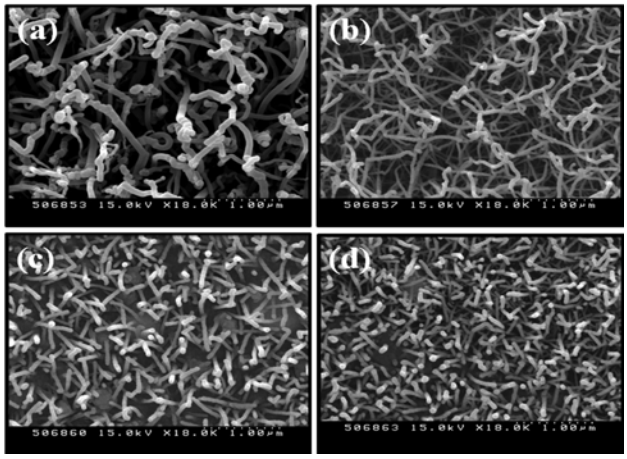

Fig. 1. SEM images of the as-synthesized products deposited on Au-coated Si substrates with Au layer thicknesses of (a) 3, (b) 10, (c) 40, and (d) 120 nm.

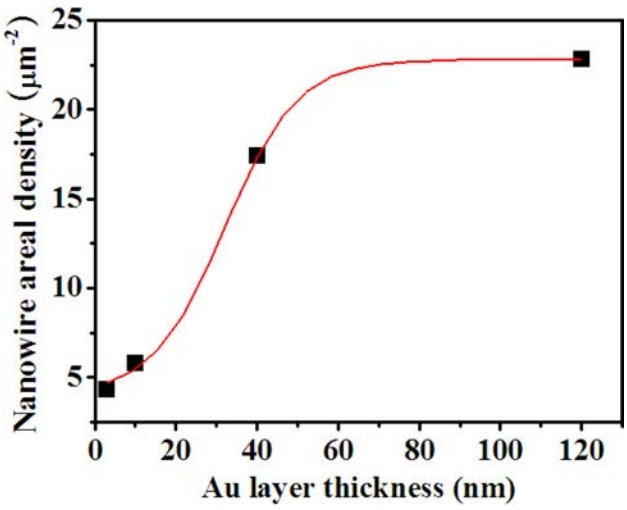

Fig. 2. Variation in the areal density of nanowires by varying the Au layer thickness.

growth process of MgO nanostructures. In the present experiment, a total constant pressure was set to about 2 torr (267 Pa). In the ambient gas, the ratio of gas flow rates of Ar and O_2 were about 97.9 and 2.1%, respectively. The substrate temperature was set to 1000 °C for 2 h.

The samples were analyzed using glancing angle (0.5°) X-ray diffraction (XRD, X'pert MPD-Philips with CuKá$_1$ radiation), scanning electron microscopy (SEM, Hitachi S-4200), and transmission electron microscopy (TEM, Philips CM-200) with an energy-dispersive X-ray (EDX) spectrometer attached. Raman spectra were taken at room temperature using a Renishaw Raman spectromicroscope in the open air at KBSI (Korea). A He-Ne laser beam with a wavelength of 633 nm was used for Raman excitation. PL was carried out in a closed-cycle helium refrigerator system at room temperature. As the excitation source, we have used the 325-nm line of a He-Cd laser at 10 mW. The luminescence signal was dispersed by a SPEX 0.55-m

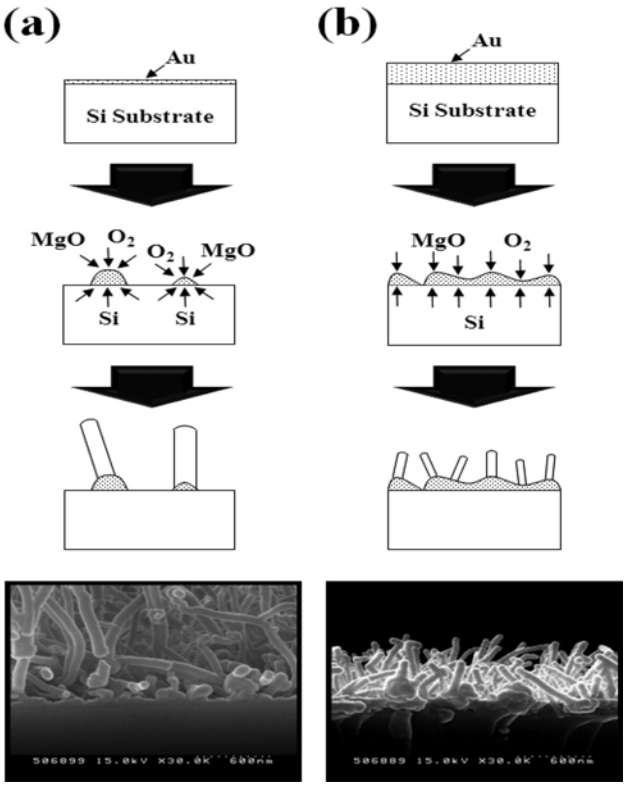

Fig. 3. Schematic outline of the synthesis of Mg_2SiO_4 nanowires with (a) thin and (b) thick Au layer. The SEM micrographs shown in (a) and (b) represent the side-view images of the nanowires with a Au layer thickness of 3 and 40 nm, respectively.

spectrometer and detected with a liquid-nitrogen-cooled back-illuminated charge-coupled-device (CCD).

Results and Discussion

Figs. 1a, 1b, 1c, and 1d show the typical SEM images deposited on Au layers with thicknesses of 3, 10, 30, and 120 nm, respectively, indicating that the products consist of a large quantity of 1D structures, regardless of the Au layer thickness. We have estimated the areal densities of nanowires by counting the number of nanowire tips from the top-view SEM images. Fig. 2 displays the variation of nanowire areal densitiy with changing Au layer thickness. Herein, the areal densities of nanowires with Au layer thicknesses of 3, 10, 40, and 120 nm are approximately 4.3, 5.8, 17.4, and 22.8 ìm^{-2}, respectively, revealing that the areal density of the Mg_2SiO_4 nanowires increased with an increase in the thickness of the predeposited Au layer.

In the present base-growth process [23], the Au layer played a catalytic role, by forming a Au-Si liquid alloy during the heating at 1000 °C. From this alloy, the nanowires can be precipitated. When the Au layer is relatively thin, the 1000 °C-heating presumably promotes the agglomeration of the Au layer, resulting in the formation of island-like structures with wide interspaces (Fig. 3a). Therefore, in the case of a thin Au

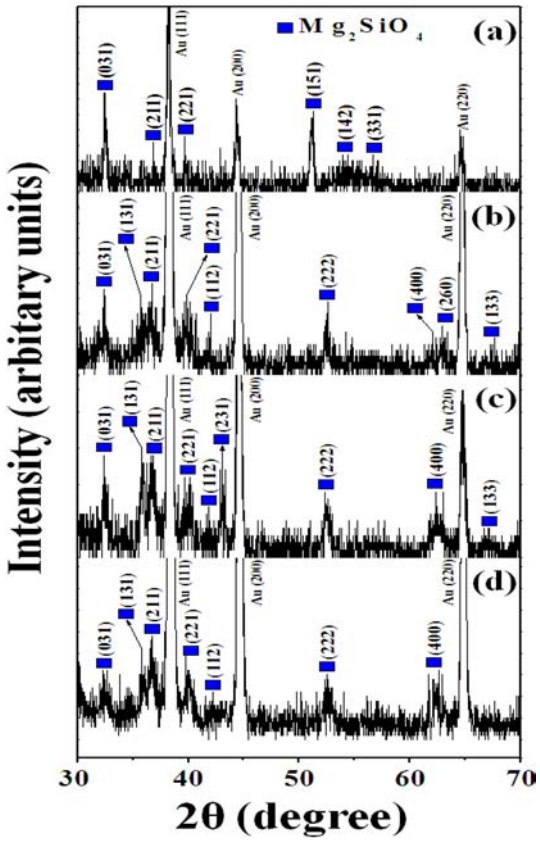

Fig. 4. XRD spectra of the as-synthesized products deposited on Au-coated Si substrates with Au layer thicknesses of (a) 3, (b) 10, (c) 40, and (d) 120 nm.

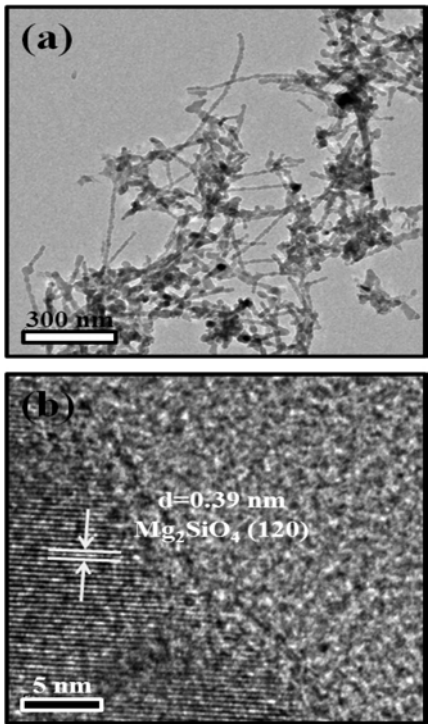

Fig. 6. Raman spectrum of as-synthesized Mg_2SiO_4 nanowires.

layer, sparse nanowires may be formed from the locally-present islands. Furthermore, the nanowires may become thicker and longer due to the concentrated flow of chemical species (Si, O, and Mg) into the sparesely localized sites. On the other hand, with 1000 °C-heating, a relatively thick Au layer cannot be transformed into small islands (Fig. 3b). In this case, a nearly omnipresent thick Au layer on the substrate surface may provide dense nucleation sites, resulting in the formation of smaller nanowires with a higher areal density.

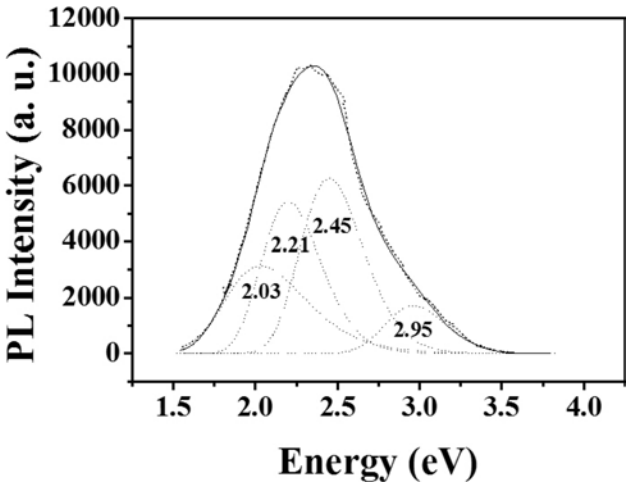

Fig. 7. PL spectrum of as-synthesized Mg_2SiO_4 nanowires. The measurement temperature was 8 K. The light source was the 325 nm-wavelength line from a He-Cd laser.

In order to confirm that the nanowires correspond to the Mg_2SiO_4 structure, we have employed the XRD and TEM analyses. Figs. 4a, 4b, 4c, and 4d show XRD spectra of the products deposited on Au layers with thicknesses of 3, 10, 30, and 120 nm, respectively. Apart from the Au-related peaks which are from the underlying substrate, nearly all recognizable reflection peaks can be readily indexed to the orthorhombic Mg_2SiO_4 structure with lattice parameters of a = 5.982 Å, b = 10.198 Å and c = 4.755 Å, which are consistent with the standard data file (JCPDS: 34-0189). Fig. 5a shows a low-magnification TEM image, revealing that the product consists of an agglomeration of 1D nanowires, agreeing with the SEM observations. Fig. 5b shows a lattice-resolved TEM image enlarging an area near a nanowire surface. The lattice fringe distance is approximately 0.39 nm, which is in coincidence with the (120) plane of orthorhombic Mg_2SiO_4 (JCPDS: 34-0189).

Fig. 6 shows the Raman spectrum of the as-prepared Mg_2SnO_4 nanowires. While the sharp peak at 520 cm^{-1} was identified as the TO phonon mode in the silicon (Si) crystal structure [24], presumably from the Si substrates, the peak centered at 941 cm^{-1} is associated with the surface phonon mode of amorphous silica, which should have been formed on the surface of Si substrate [25]. Besides, in the 941 cm^{-1}-centered broad band, we suppose that there exists a $B_{1u}{}^b$ IR active

mode, which is usually observed at a vibrational frequency of 978 cm^{-1}, which is related to the internal SiO_4 mode [26]. The prominent Raman line at 303 cm^{-1} can be assigned to the A_g Raman active mode of the SiO_4 group from Mg_2SnO_4 [26]. In addition, the weak Raman line at 432 cm^{-1} coincides with the B_{2g} Raman internal SiO_4 mode of Mg_2SnO_4 [26]. The line at 823 cm^{-1} coincides with the A_g Raman active [26,27] (internal SiO_4) mode. Also, the weak Raman line at 620 cm^{-1} coincides with the B_{2g} Raman active (internal SiO_4) mode [26].

In order to precisely evaluate the optical properties of Mg_2SnO_4 nanowires, we have investigated the PL spectrum measured at a very low temperature. A PL spectrum of as-synthesized Mg_2SnO_4 nanowires measured at 8 K is presented in Fig. 7. In order to have closer insights to the origin of the broad emission band which can be a superimposition of several peaks, we have fitted the spectral feature with Gaussian functions. The best fit of the emission was obtained with four Gaussian functions, which are centered at 2.03, 2.21, 2.45, and 2.95 eV. Since there has been rare reports on the PL of Mg_2SiO_4, the origin of these emission bands are not clear. Furthermore, the luminescence from pure Mg_2SiO_4 has not been reported so far. Accordingly, it is surmised that the luminescence from the present Mg_2SiO_4 nanowires originated from defects and/or impurities.

Koike et al. reported the thermoluminescence (TL) spectra of Mg_2SiO_4 single crystals [28,29]. It is revealed that the PL spectrum is similar to that of the TL spectra [30]. The TL spectra are comprised of blue (2.8-3.0 eV) and red emission bands (1.9 eV) [28,29]. The red emission of the 2.03 eV-peak in the present study can originate from minor trace elements in Mg_2SiO_4 nanowires [29]. Since the blue emission in the TL of Mg-comprising cosmic matter is related to the isotopes [30], we surmise that the blue emission from the present Mg_2SiO_4 nanowires is attributed to impurities. In addition, intermediate peaks centered at 2.21 and 2.45 eV are observed in Fig. 7. Although there is a rare report on a similar emission, Shinno et. al presented the luminescence of mechanically-shocked Mg_2SiO_4 single crystals in the range of 2.04-2.95 eV [31]. Accordingly, it is surmised that the 2.21 eV- and 2.45 eV-centered peaks are ascribed to the Mg_2SiO_4 structure.

Conclusions

We have synthesized Mg_2SiO_4 nanowires by heating Au-coated Si substrates at 1000 °C. During heating, Mg-related vapors were incorporated from the inner surface of the quartz tube. The thickness of the Au layer on the Si substrate significantly affected the wire morphology, where the areal densities of the Mg_2SiO_4 nanowires increased with an increase in the thickness of the predeposited Au layer. We suggest that the thick predeposited Au layer will provide dense nucleation sites, resulting in the formation of smaller nanowires with a higher areal density. XRD spectra and lattice-resolved TEM images coincidentally reveal that the nanowires correspond to orthorhombic Mg_2SiO_4 structures. In the Raman spectrum, the Raman lines at 303, 432, 620, and 823 cm^{-1} was related to the SiO_4 group from Mg_2SnO_4. The PL measurements with Gaussian fitting show apparent visible light emission bands centered at 2.03, 2.21, 2.45, and 2.95 eV. The red (2.03 eV) and blue (2.95 eV) emissions are attributed to impurities in the Mg_2SiO_4 nanowires.

Acknowledgements

This work was supported by the research fund of Hanyang University (HY-2011-201100000000434).

References

1. H.Y. Yang and T.W. Kim, J. Ceram. Proc. Res. 11 (2010) 769-772.
2. C.S. Lim, J.H. Ryu, D.-H. Kim, S.-Y. Cho and W.-C. Oh, J. Ceram. Proc. Res. 11 (2010) 736-741.
3. F.A. Sheikh, M.A. Kanjwai, H. Kim, D.R. Pandeya, S.T. Hong and H.Y. Kim, J. Ceram. Proc. Res. 11 (2010) 685-691.
4. K.-S. Yun and C.-J. Park, Electron. Mater. Lett. 6 (2010) 173-176.
5. C. Hong, H. Kim, H.W. Kim and C. Lee, Met. Mater. Int. 16 (2010) 311-315.
6. H.W. Kim, H.S. Kim, M.A. Kebede, H.G. Na and J.C. Yang, Met. Mater. Int. 16 (2010) 77-81.
7. Y.-S. Kim, K.-C. Kim and T.-W. Hong, Met. Mater. Int. 16 (2010) 225-228.
8. D.Y. Lee, M.-H. Lee, N.-I. Cho, B.-Y. Kim and Y.-J. Oh, Met. Mater. Int. 16 (2010) 453-457.
9. C.M. Choi, Y.C. Yoon, D.H. Hong, K.S. Brammer, K.B. Noh, Y. Oh, S.H. Oh, F.E. Talke and S.H. Jin, Electron. Mater. Lett. 6 (2010) 59-65.
10. S.G. Shin, Electron. Mater. Lett. 6 (2010) 65-71.
11. X.F. Duan, Y. Huang, Y. Cui, J. Wang and C.M. Lieber, Nature 409 (2001) 66-69.
12. M.H. Huang, S. Mao, H. Feick, H.Q. Yan, Y.Y. Wu, H. Kind, E. Weber, R. Russo and P.D. Yang, Science 292 (2001) 1897-1899.
13. V. Petricevic, S.K. Gayen and R.R. Alfano, Appl. Phys. Lett. 52 (1988) 1040-1042.
14. H.R. Verdun, L.M. Thomas, D.M. Andrauskas and T. Mccolium, Appl. Phys. Lett. 53 (1988) 2593-2595.
15. J. Lazewski, P.T. Jochym, K. Parlinski and P. Piekarz, J. Mol. Struct. 596 (2001) 3-6.
16. T. Ban, Y. Ohya and Y. Takahashi, J. Am. Ceram. Soc. 82 (1999) 22-26.
17. M.B.D. Mitchell, D. Jackson and P.F. James, J. Non-Cryst. Solids 225 (1998) 125-129.
18. A.E. Kimaev, M.V. Korzhik, M.G. Livshits, B.I. Minkov, Ya.I. Mishkel and A.A. Tarasov, Opt. Spectrosc. 70 (1991) 415-416.
19. T. Tani and S. Saeki, J. Am. Ceram. Soc. 90 (2007) 805-808.

20. Z. Zhang, L.M. Wong, H.X. Wang, Z.P. Wei, W. Zhou, S.J. Wang and T. Wu, Adv. Funct. Mater. 20 (2010) 2511-2518.
21. S. Xie, W. Zhou and Y. Zhu, J. Phys. Chem. B 108 (2004) 11651-11566.
22. R.L.D. Whitby, K.S. Brigatti, I.A. Kinloch, D.P. Randall and T. Maekawa, Chem. Commun. (2004) 2396-2397.
23. H.W. Kim and S.H. Shim, Appl. Phys. A 86 (2007) 361-364.
24. M. Hirasawa, T. Orii and T. Seto, Appl. Phy. Lett. 88 (2006) 093119.
25. Y.D. Glinka and M. Jaroniec, J. Appl. Phys. 82 (1997) 3499-3507.
26. V. Devarajan and E. Funck, J. Chem. Phys. 62 (1975) 3406-3411.
27. J.L. Servoin and B. Piriou, Phys. Stat. Sol. (b) 55 (1973) 677-686.
28. K. Koike, M. nakagawa, C. Koike, M. Okada and H. Chihara, Astron. Astrophys. 390 (2002) 1133-1139.
29. C. Koike, H. Chihara, K. Koike, M. Nakagawa, M. Okada, A. Tsuchiuama, M. Aoki, T. Atawa and K. Atobe, Meteorit. Planet Sci. 37 (2002) 1591-1598.
30. K. Koike, M. Nakamura, C. Koike, H. Chihara, M. Okada, M. Matsumura, T. Awata and K. Atobe, J. Takada, Planet. Space Sci. 54 (2006) 325-330.
31. I. Shinno, T. Nakamura and T. Sekine, J. Lumin. 87-89 (2000) 1292-1294.